Synthesis of Superconducting Cobalt Trihydride

Synthesis of Superconducting Cobalt Trihydride

Miriam Peña-Alvarez,[*,†] Bin Li,[‡,¶] Liam C. Kelsall,[†] Jack Binns,[§] Philip Dalladay-Simpson,[§] Andreas Hermann,[†] Ross T. Howie,[§] and Eugene Gregoryanz[*,§,†]

†*Centre for Science at Extreme Conditions & The School of Physics and Astronomy, The University of Edinburgh, Peter Guthrie Tait Road, Edinburgh, U.K.*

‡*National Laboratory of Solid State Microstructures, Nanjing University, Nanjing 210093, China*

¶*New Energy Technology Engineering Laboratory of Jiangsu Province and School of Science, Nanjing University of Posts and Telecommunications, Nanjing 210023, China*

§*Center for High Pressure Science & Technology Advanced Research, 1690 Cailun Road, Shanghai, 201203, China*

E-mail: mpenaal@ed.ac.uk; e.gregoryanz@ed.ac.uk

High pressure, cobalt, hydrogen, cobalt hydride, X-ray diffraction, Density Functional Theory

Abstract

The Co-H system has been investigated through high-pressure high-temperature x-ray diffraction experiments combined with first principles calculations. On compression of elemental cobalt in a hydrogen medium, we observe *fcc* cobalt hydride (CoH) and cobalt dihydride (CoH_2) at 33 GPa. Laser heating CoH_2 in a hydrogen matrix at 75 GPa to temperatures in excess of $\sim$ 800 K, produces cobalt trihydride (CoH_3) which adopts a primitive structure. Density functional theory calculations support the stability of CoH_3. This phase is predicted to be thermodynamically stable at pressures above 18 GPa and to be a superconductor below 23 K as critical temperature, T_c. Theory predicts that this phase remains dynamically stable upon decompression above 11 GPa where it has a maximum T_c of 30 K.

Graphical TOC Entry

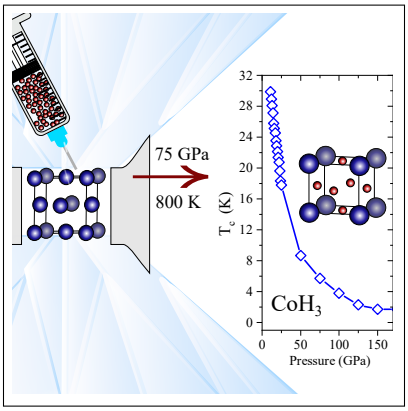

The physical properties of a host metal can be profoundly altered by the presence of hydrogen. Metallic structures have been predicted that when hosting high density atomic hydrogen they could exhibit novel properties such as high-temperature superconductivity.[1] The potentials of these materials are exemplified by the recent high-temperature superconductivity experimentally observed in the rare-earth hydrides.[2,3] Prior to these findings, superconductivity was also proposed to emerge in the transition metal hydrides (TMH).[4–6]

The transition metals are good electron donors, as they tend to donate their two external s^2 electrons thus stabilizing the H^- anion over molecular hydrogen. Under moderate pressures, almost all transition metals form monohydride compounds.[7–9] Platinum, for example, is observed to form two hexagonal monohydride variants, PtH-I and PtH-II, at pressures above 27 GPa.[10] *Ab initio* calculations initially predicted PtH-II to be a superconductor, with a critical temperature, T_c, below 17 K at 90 GPa, however with the inclusion of anharmonic effects, the T_c was substantially reduced to < 1 K.[5,10,11] Recent electrical measurements found that at 30 GPa, PtH-II has a T_c of 7 K, which reduced on further compression.[12] Through a combination of high pressure and/or high temperature, TMH with more unusual stochiometries become energetically competitive.[13–22] Iron exhibits several polyhydride species, of which FeH_5 ($I4/mmm$), synthesised at 120 GPa and temperatures >1500 K, is the most hydrogen-rich and possesses a unique layered structure.[23] Potential superconductivity in FeH_5 has been a subject of debate, with two theoretical works predicting remarkably high T_c values ranging between 46 - 51 K, and conversely, another computational study finding no superconductivity.[24–26] However, the latter study did suggest that trihydrides heavier than FeH_3, with a cubic $Pm\bar{3}m$ structural type, could facilitate superconductivity through the addition d electrons to the hybrid $3d$ electron shell of the metal-hydrogen band.[26]

Cobalt is a prime transition metal candidate to also exhibit a trihydride form, being positioned in the same group as iridium and period neighbour iron, both of which form cubic trihydrides.[14,23] Indeed, a recent theoretical study predicted the formation of CoH_3 above 30 GPa sharing the same $Pm\bar{3}m$ structure as both FeH_3 and IrH_3.[27] However, both

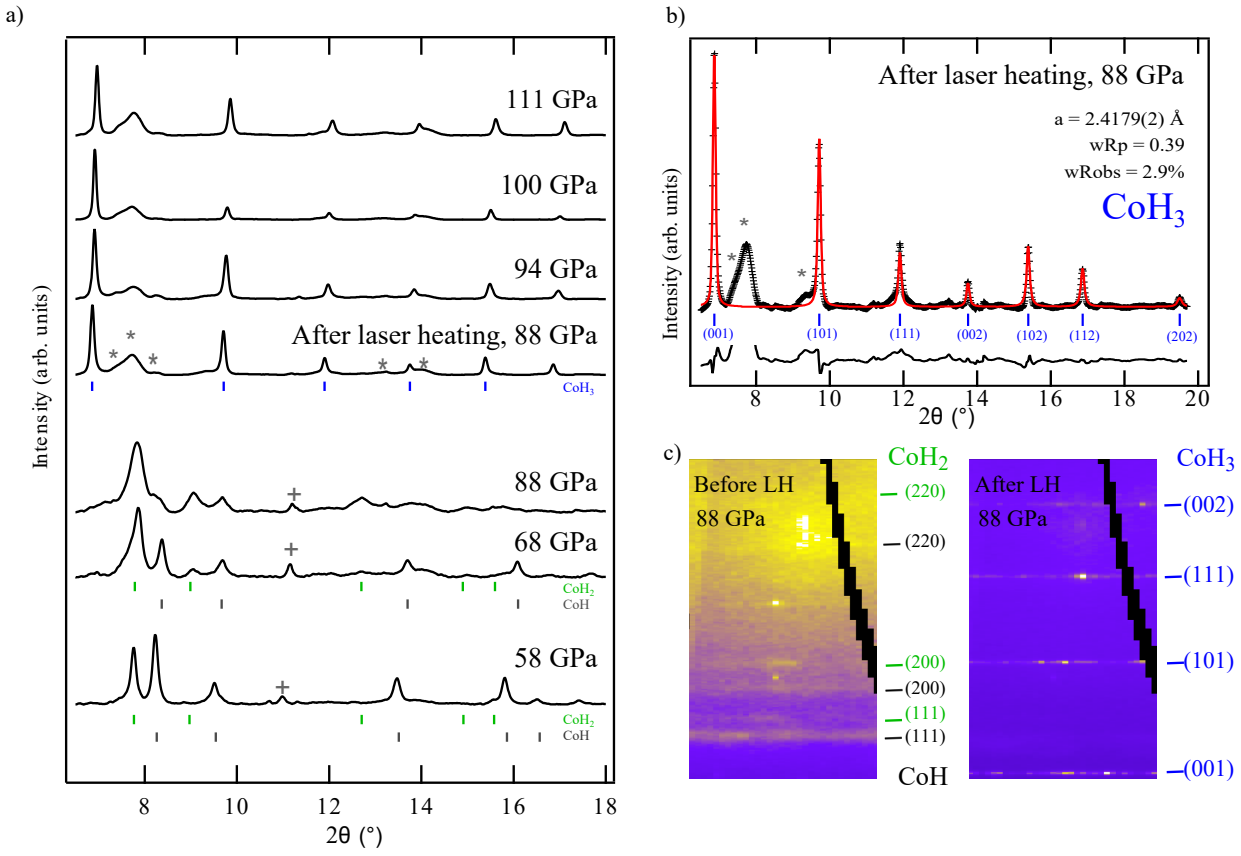

Figure 1: (a) High pressure x-ray diffraction patterns ($\lambda = 0.2895$ Å) taken on compression to 111 GPa. Laser heating at 88 GPa yields the synthesis of $Pm\bar{3}m$ cobalt trihydride.Asterisks correspond to Re and ReH, whilst crosses correspond to W. (b) Rietveld refinement fit of CoH_3 structures, unfitted peaks marked by $*$ correspond to ReH and Re. Refinement parameter are wRp=0.39 and wR_{obs}=2.9. (c) Diffraction plates of the sample at 88 GPa before (left) and after (right) laser heating. In all panels, tick marks indicate the reflections of CoH (grey), CoH_2 (green), CoH_3 (blue).

these studies and a further computational work, predict CoH_3 to have a T_c below 1 K at pressures above 150 GPa.[26,27] Experimentally, the synthesis of CoH_3 has remained elusive, with only the formation of face-centred cubic CoH above 4 GPa and the stepwise transition to CoH_2 above 45 GPa.[20]

Here, we demonstrate the synthesis of cobalt trihydride in a laser-heated diamond-anvil cell through a series of synchrotron X-ray diffraction experiments. On compression, we observe the known formation of both CoH and CoH_2, which we find to co-exist to at least 75 GPa. Laser heating CoH and CoH_2 in a hydrogen matrix at pressures and temperatures above 75 GPa and 700 K leads to the complete transformation of the sample, identified by new diffraction peaks. We identify the new compound as CoH_3 and find it to be isostructural to FeH_3, with Co atoms occupying the vertices of the simple cubic unit cell and H atoms occupying the vacant face centers.[15] Total energy and electron-phonon calculations reveal that CoH_3 remains energetically stable down to 18 GPa, at which pressure it exhibits superconductivity with a T_c of 23 K.

After gas loading at 0.2 GPa, mixtures of Co and H_2 were compressed to 33 GPa. After one week at this pressure, x-ray diffraction patterns reveal the synthesis of both CoH and CoH_2 compounds, in agreement with previous work.[20] CoH has space group symmetry $Fm\bar{3}m$, with unit-cell length $a = 3.4849(7)$ Å (at 60 GPa), while CoH_2 has unit cell length $a = 3.7533(8)$ Å (at 60 GPa) within the same group. Interestingly, CoH_2 is not isostructural to FeH_2 which adopts a tetragonal $I4/mmm$ structure,[15] but instead adopts the same structure as RhH_2 at 14 GPa.[13] Remarkably, we find that both CoH and CoH_2 co-exist up to pressures of 88 GPa (see Figure 1(a)), with no indication of further hydrogenation. We also do not observe a transition on compression to tetragonal ($I4/mmm$) CoH_2, which was predicted to become energetically favourable above 42 GPa.[27]

The laser heating of metals in a high-pressure hydrogen environment has been a successful synthetic tool in yielding hydrogen-rich metal hydrides,[3,17,30,31] and was utilised here to explore the synthesis of cobalt polyhydride species. Samples of CoH/CoH_2 and H_2 were

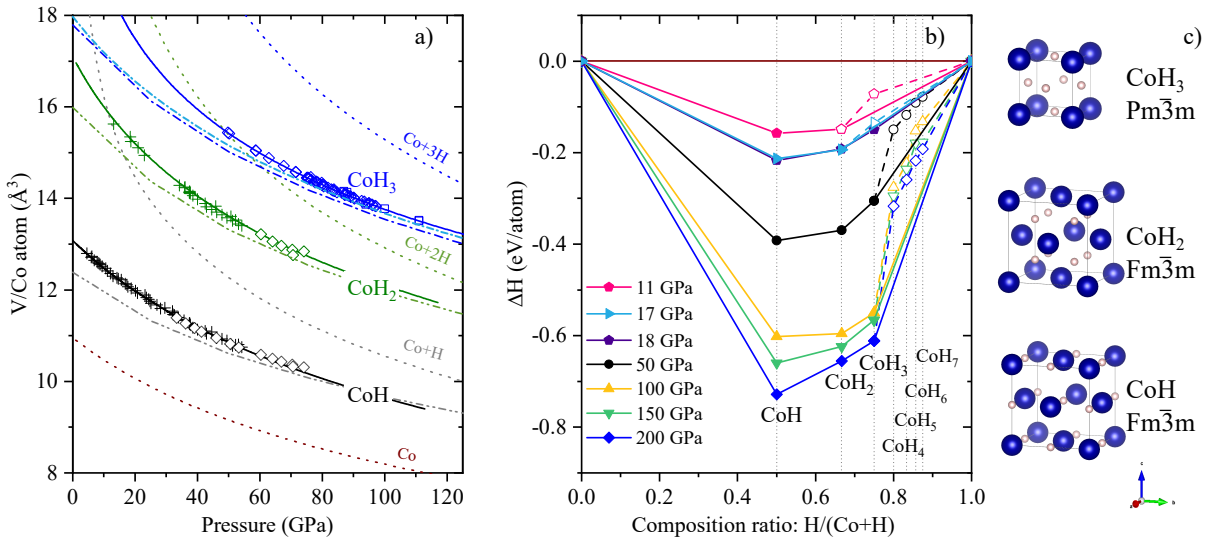

Figure 2: (a) Volume per Co atom for Co-H compounds. Diamond and square symbols correspond to measurements from two experimental runs, whilst crosses represent data taken from Wang et al.[20] Solid lines correspond to the experimental equation of states (EOS) calculated using data from this work and Wang *et al.*.[20] Dashed dotted lines were calculated through DFT using ultrasoft pseudopotentials (QuantumESPRESSO code). For CoH_3 the light blue dashed-dotted line was calculated with VASP, using 'hard' PAW pseudopotentials and the optB88-vdW dispersion-corrected functional. Dotted lines represent the EOS derived from the atomic volumes of Co and H.[28,29] (b) Convex hull construction for CoH_x compounds at a sequence of pressures. Empty (filled) symbols denote metastable (stable) phases. (c) Crystal structures of cobalt polyhydrides, CoH ($Fm\bar{3}m$), CoH_2 ($Fm\bar{3}m$) and CoH_3 ($Pm\bar{3}m$). Co atoms are represented by blue spheres and H atoms are represented by pink spheres.

compressed to pressures of 75 GPa and 88 GPa, and held here for 24 and 12 hours respectively, observing no time induced transformation. These samples were then laser heated to about <800 K (Figure S1 and see methods for further details). Upon quenching of the sample, we see the disappearance of the diffraction lines attributed to CoH/CoH_2, which are supplanted by new diffraction peaks (see Figure 1(a,c) and S1[32]). All of the new diffraction peaks can be indexed with a simple cubic unit cell ($Pm\bar{3}m$) with lattice parameter a = 2.4358(2) Å at 75 GPa. Rietveld refinements of this structure (Figure 1(b)) show Co atoms to be on the vertexes of the unit cell, with final agreement factors of wRp 0.39 and a wR_{obs} 2.9. Samples were compressed up to 111 GPa, the highest pressure reached in this study, and subsequently decompressed down to 52 GPa (below which the sample was lost due to anvil failure) to determine the equation of state (EoS) and evaluate the stability of the compound. The volume per Co atom as a function of pressure of CoH, CoH_2, and the synthesised product were fitted with third-order Birch-Murnaghan P-V EoS's (see Figure 2 (a)) with the fit parameters shown in table S1. The experimentally determined EoS gives volumes greater than Co+2H, and comparison between the experimental EOS and that determined theoretically for CoH_3 present a good agreement. The determined structure also matches that of which was previously predicted for CoH_3,[27] and is isostructural to FeH_3,[15] synthesised through similar methods.

We have performed our own variable-composition structure search to find energetically stable structures in the Co-H system up to 400 GPa using the evolutionary crystal structure prediction method USPEX package and the particle swarm optimisation method as implemented in the CALYPSO code (Figures S2-S4).[33–37] Through enthalpy calculations for the most stable structures, we find CoH_3 to adopt a $Pm\bar{3}m$ unit cell identical to FeH_3[15,38] and IrH_3,[14] with the H atoms occupying the 3c site $(0, \frac{1}{2}, \frac{1}{2})$. This, together with the computationally determined EOS, is in good agreement with experiments. CoH_3 is on the convex hull above 18 GPa, , however experimentally we only see CoH and CoH_2 which we attribute to kinetics barriers. CoH and CoH_2 have the highest formation enthalpies, 0.602 and 0.596 eV

per atom respectively at 100 GPa (see Figure 2) and also share the same *fcc*-Co sub lattice. Pure Co adopts a *hcp* phase at pressures below 105 GPa, above which it transforms to *fcc*-Co.[29] So although *fcc*-Co is not the ground state at 33-55 GPa, it is likely there is a low energy barrier[39] to form metastable *fcc*-Co, which can then be filled with hydrogen to form CoH and/or CoH_2. Experimentally, both compounds can be formed on compression alone, with laser heating accelerating the process.[20]

CoH_3, however, is very different, as it has a *simple cubic* Co sub lattice. Since it is not close packed a major rearrangement of the Co lattice is required to allow the formation of CoH_3. Neither low pressure and high temperature or long times at pressures below 50 GPa are sufficient to initiate the CoH_3 formation,[20] requiring pressures above 75 GPa and laser heating to trigger the CoH_3 synthesis. In agreement with the convex hull calculations, and Gibbs' phase rule, only CoH_3 is formed after the laser heating in an excess H_2 environment. Our DFT calculations also find an unreported structural transition in CoH_2 above 275 GPa to a tetragonal $P4/nmm$ phase (Figure S4).

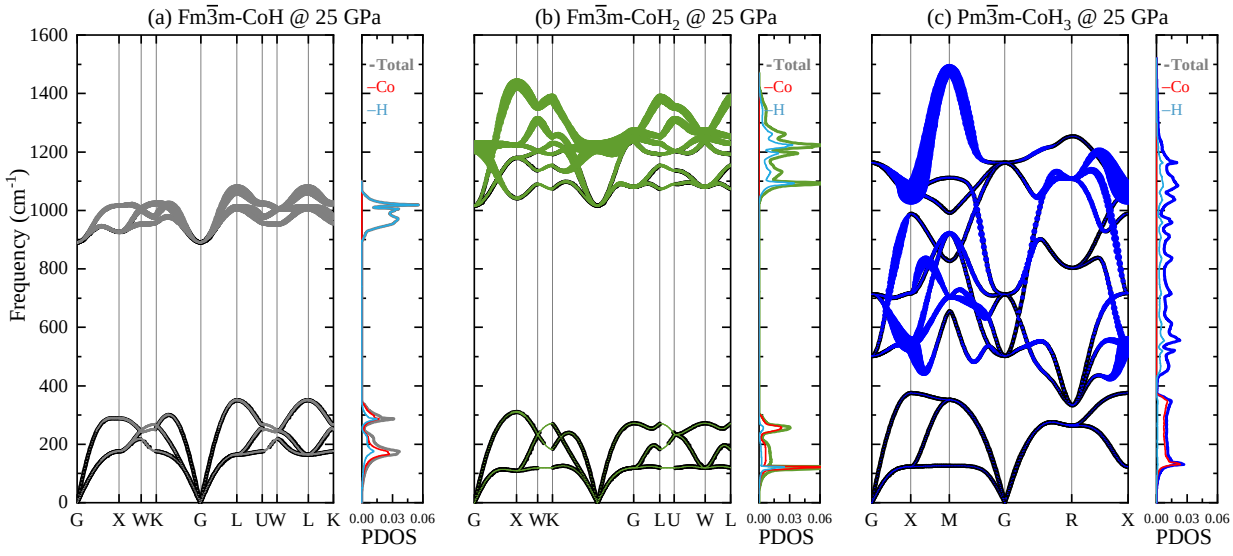

Figure 3: Phonon dispersion curves and Projected phonon density of states at at 25 GPa for; (a) CoH, (b) CoH_2, (c) CoH_3. The phonon dispersions $\omega_\nu(\mathbf{q})$ for each phonon mode ν at momentum space point $\mathbf{q}$ are drawn as circles with radii proportional to the magnitude of the electron-phonon linewidths $\gamma_{\mathbf{q}\nu}$.

Recent theoretical work anticipated that transition metal trihydrides isostructural to

FeH_3 but with heavier elements, like Co, would be candidates to undergo superconducting transitions.[26] Our DFT calculations of the electronic structure and electronic bands demonstrate metallicity of the three hydrides at all pressures throughout their stability ranges (see Figure S5 - S8). At the lowest pressure, the electronic density of states (DOS) of CoH_3 (see Fig. S5) has important contributions from hydrogen orbitals around the Fermi level, indicative that it could exhibit superconductivity.

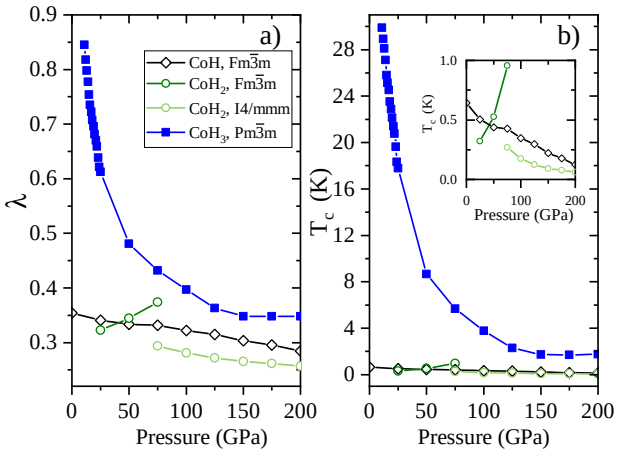

Figure 4: (a) Electron-phonon coupling constant λ for the calculated favoured cobalt hydrides phases as a function of pressure. (b) Critical temperature, T_c, for CoH, CoH_2 and CoH_3 as a function of pressure. Insert shows T_c as a function of pressure between 0 and 1 K. In all panels, CoH is represented as black diamonds, CoH_2 as green circles and CoH_3 as blue squares.

In Figure 3 we show the calculated phonon dispersion curves and projected phonon density of states (PDOS) for the low pressure phases of CoH, CoH_2 and CoH_3 at 25 GPa (see Figures S9-S12 for higher and lower pressure results). Phonon structures of all the hydrides depict no imaginary frequencies along the high symmetry k path, which demonstrates their dynamical stability. For $Fm\bar{3}m$-CoH, as shown in Figure 3(a), a phonon gap between 400 cm^{-1} and 900 cm^{-1} divides the spectrum into two regions: the low-frequency acoustic branches and high-frequency optical branches. The optical modes are associated with almost exclusive motion of H atoms, whereas the acoustic modes are associated with the concerted motions of both Co and H atoms. From Figure 3(b), CoH_2 has a similar gapped phonon

spectrum compared to CoH, but with higher optical frequency branches up to 1400 cm^{-1} in the hydrogenic sublattice. In CoH_3, there is a big change in the phonon dispersion and PDOS. The phonon gap has shrunk and the larger number of optical branches occupies a much wider frequency region. From CoH to CoH_3, the magnitude of the electron-phonon linewidths increases with the higher hydrogen content, which may lead to a higher zone-averaged electron-phonon coupling parameter (EPC) and superconducting critical temperature, T_c.

We estimate the EPC and T_c using the McMillan-Allen-Dynes formula[40–42]

$$T_c = \frac{\omega_{ln}}{1.2} \exp\left[-\frac{1.04(1+\lambda)}{\lambda - \mu^*(1+0.62\lambda)}\right], \quad (1)$$

where ω_{ln} is the logarithmically averaged phonon frequency, and taking the Coulomb parameter as $\mu^* = 0.1$. The EPC λ and T_c are plotted in Figure 4 as a function of pressure. For CoH and CoH_2, the calculated λ are below ~ 0.45 in the studied pressure range. Such weak EPC result in T_c below 2 K. However, as seen in Figure 4, CoH_3 shows a different and remarkable trend with λ significantly increased with decreasing pressure, which in turn leads to a rapid T_c increase upon decompression, reaching a predicted maximum of 30 K at 11 GPa.

There are some quantitative differences between our results and those obtained in previous calculations.[27] For CoH_3 at 200 GPa we obtain $\lambda = 0.35$ and $T_c = 2$ K, while Wang *et al.*[27] obtain $\lambda = 0.19$ and $T_c \sim 0$ K. We have repeated our calculations with parameters very similar to those used by Wang *et al.* (see figs. S13-S23) and reproduce the EPC and T_c data (Figure S23, $\lambda = 0.21$ and $T_c = 4$ mK). We postulate that the choice of pseudopotential – norm-conserving (NC) in Wang *et al.*[27] and ultrasoft (US) here – is the source of the quantitative differences we see. The US pseudopotentials are better suited than the NC to describe the EOS of pure Co and H[43] but give very similar EOS results for CoH_3; both also agree with VASP calculations using the PAW method, see Figure S13 in the SM. The choice of pseudopotential has a larger effect on phonon properties than on electronic properties;

Nonetheless, using either approach, the EPC and T_c share the same trend upon compression, but on different absolute scales (see Figure S23) - with the NC pseudopotentials, a T_c of CoH_3 is predicted to reach 15 K at 13 GPa the US pseudopotentials give the same value if the screened Coulomb interaction μ^* would be increased to 0.18). These quantitative uncertainties might be best resolved by using more sophisticated theoretical approaches such as directly solving the Eliashberg equation or the superconducting DFT method.[44,45]

The strong negative pressure dependence of T_c in CoH_3 at these low pressures can be explained by the hardening of the phonon frequencies leading to a weakening of EPC λ. As shown in Figures 3 and S9-S12, when the pressure increases from 10 GPa to 300 GPa, the maximal frequencies of optical phonon branches for CoH_3 hardens from 1500 cm^{-1} to 2400 cm^{-1}, while DOS $N(0)$ (see figures S6 to S8) and magnitude of electron-phonon linewidths $\gamma_{\nu q}$ remain almost unchanged. A similar trend in T_c was experimentally observed in PtH-II, from 7 K at 30 GPa to 5 K at 40 GPa.[12]

In our experimental runs, diamond failure on decompression prevented us to study the stability of CoH_3 at pressures lower than 52 GPa. At 52 GPa, we predict CoH_3 to have T_c of 8 K, which could increase to 30 K at 11 GPa. We speculate that due to the large stability range predicted for CoH_3 (Figure S1), that low temperature could maintain the stability of CoH_3 down to it's maximal T_c conditions, and such behaviour should be explored in future studies.

The predicted superconducting character of CoH_3 proves that TMH_3 heavier than FeH_3 do facilitate more efficient electron-phonon coupling. We have demonstrated the formation of CoH_3 synthesised at 75 GPa and stable in decompression to at least 52 GPa. CoH_3 adopts a cubic $Pm\bar{3}m$ structure which is very stable both in compression up to 111 GPa and in decompression down to 52 GPa. Our DFT results predict that this structure should be superconducting with a T_c which increased with decreasing pressure, reporting a maximum of 30 K at 11 GPa. These results give a an indication that superconductivity could also be observed in metal hydrides at low pressure conditions.

Acknowledgement

MPA would like to acknowledge the support of the European Research Council (ERC) Grant "Hecate" reference No. 695527 held by Prof. G. J. Ackland. RTH would like to acknowledge the support of the National Science Foundation of China (Grant No. 11974034). Portions of this work were performed at GeoSoilEnviroCARS (The University of Chicago, Sector 13), Advanced Photon Source (APS), Argonne National Laboratory. GeoSoilEnviroCARS is supported by the National Science Foundation - Earth Sciences (EAR - 1634415) and Department of Energy - GeoSciences (DE-FG02-94ER14466). We acknowledge DESY (Hamburgh, German) a member of the Helmholtz Association HGF, for the provision of experimental facilites. Parts of this research were carried out at PETRA-III, and we would like to thank H.-P. Liermann and. N. Giordiano for assistance in using beamline P02.2 (I-20191366). This research used resources of the Advanced Photon Source, a U.S. Department of Energy (DOE) Office of Science User Facility operated for the DOE Office of Science by Argonne National Laboratory under Contract No. DE-AC02-06CH11357. Computational resources provided by the UK's National Supercomputer Service through the UK Car-Parrinello consortium (EP/P022561/1) and project ID d56 'Planetary Interiors' and by the UK Materials and Molecular Modelling Hub (EP/P020194) are gratefully acknowledged.

Supporting Information Available

The Supporting Information is available free of charge at `https://`

- Experimental and theoretical methods
- Equation of state parameters, electronic and phonon band structures, experimental and calculated unit-cell parameters.

References

(1) Ashcroft, N. Hydrogen dominant metallic alloys: high temperature superconductors? *Physical Review Letters* **2004**, *92*, 187002.

(2) Drozdov, A.; Kong, P.; Minkov, V.; Besedin, S.; Kuzovnikov, M.; Mozaffari, S.; Balicas, L.; Balakirev, F.; Graf, D.; Prakapenka, V. et al. Superconductivity at 250 K in lanthanum hydride under high pressures. *Nature* **2019**, *569*, 528.

(3) Somayazulu, M.; Ahart, M.; Mishra, A. K.; Geballe, Z. M.; Baldini, M.; Meng, Y.; Struzhkin, V. V.; Hemley, R. J. Evidence for Superconductivity above 260 K in Lanthanum Superhydride at Megabar Pressures. *Physical Review Letters* **2019**, *122*, 27001.

(4) Scheler, T.; Degtyareva, O.; Gregoryanz, E. On the effects of high temperature and high pressure on the hydrogen solubility in rhenium. *The Journal of Chemical Physics* **2011**, *135*, 214501.

(5) Kim, D. Y.; Scheicher, R. H.; Pickard, C. J.; Needs, R.; Ahuja, R. Predicted formation of superconducting platinum-hydride crystals under pressure in the presence of molecular hydrogen. *Physical Review Letters* **2011**, *107*, 117002.

(6) Gao, G.; Hoffmann, R.; Ashcroft, N. W.; Liu, H.; Bergara, A.; Ma, Y. Theoretical study of the ground-state structures and properties of niobium hydrides under pressure. *Physical Review B* **2013**, *88*, 184104.

(7) Antonov, V. Phase transformations, crystal and magnetic structures of high-pressure hydrides of d-metals. *Journal of Alloys and Compounds* **2002**, *330*, 110–116.

(8) Baranowski, B. High Pressure Research on Palladium-Hydrogen Systems. *Platinum Metals Review* **1972**, *16*, 10–15.

(9) Kuzovnikov, M.; Tkacz, M. High pressure studies of cobalt–hydrogen system by X-ray diffraction. *Journal of Alloys and Compounds* **2015**, *650*, 884–886.

(10) Scheler, T.; Degtyareva, O.; Marqués, M.; Guillaume, C. L.; Proctor, J. E.; Evans, S.; Gregoryanz, E. Synthesis and properties of platinum hydride. *Physical Review B* **2011**, 214106.

(11) Errea, I.; Calandra, M.; Mauri, F. Anharmonic free energies and phonon dispersions from the stochastic self-consistent harmonic approximation: Application to platinum and palladium hydrides. *Physical Review B* **2014**, *89*, 064302.

(12) Matsuoka, T.; Hishida, M.; Kuno, K.; Hirao, N.; Ohishi, Y.; Sasaki, S.; Takahama, K.; Shimizu, K. Superconductivity of platinum hydride. *Physical Review B* **2019**, *99*, 144511.

(13) Li, B.; Ding, Y.; Kim, D. Y.; Ahuja, R.; Zou, G.; Mao, H.-K. Rhodium dihydride (RhH2) with high volumetric hydrogen density. *Proceedings of the National Academy of Sciences* **2011**, *108*, 18618–18621.

(14) Scheler, T.; Marqués, M.; Konôpková, Z.; Guillaume, C. L.; Howie, R. T.; Gregoryanz, E. High-Pressure Synthesis and Characterization of Iridium Trihydride. *Physical Review Letters* **2013**, *111*, 215503.

(15) Pépin, C. M.; Dewaele, A.; Geneste, G.; Loubeyre, P.; Mezouar, M. New Iron Hydrides under High Pressure. *Physical Review Letters* **2014**, *113*, 265504.

(16) Liu, G.; Besedin, S.; Irodova, A.; Liu, H.; Gao, G.; Eremets, M.; Wang, X.; Ma, Y. Nb-H system at high pressures and temperatures. *Physical Review B* **2017**, *95*, 104110.

(17) Binns, J.; Donnelly, M.-E.; Wang, M.; Hermann, A.; Gregoryanz, E.; Dalladay-Simpson, P.; Howie, R. T. Synthesis of Ni 2 H 3 at high temperatures and pressures. *Physical Review B* **2018**, *98*, 140101.

(18) Ying, J.; Liu, H.; Greenberg, E.; Prakapenka, V. B.; Struzhkin, V. V. Synthesis of new nickel hydrides at high pressure. *Physical Review Materials* **2018**, *2*, 085409.

(19) Marizy, A.; Geneste, G.; Loubeyre, P.; Guigue, B.; Garbarino, G. Synthesis of bulk chromium hydrides under pressure of up to 120 GPa. *Physical Review B* **2018**, *97*, 184103.

(20) Wang, M.; Binns, J.; Donnelly, M.-E.; Peña-Alvarez, M.; Dalladay-Simpson, P.; Howie, R. T. High pressure synthesis and stability of cobalt hydrides. *The Journal of Chemical Physics* **2018**, *148*, 144310.

(21) Ying, J.; Li, X.; Greenberg, E.; Prakapenka, V. B.; Liu, H.; Struzhkin, V. V. Synthesis and stability of tantalum hydride at high pressures. *Physical Review B* **2019**, *99*, 224504.

(22) Binns, J.; He, Y.; Donnelly, M.-E.; Peña-Alvarez, M.; Wang, M.; Kim, D. Y.; Gregoryanz, E.; Dalladay-Simpson, P.; Howie, R. T. Complex Hydrogen Substructure in Semimetallic RuH4. *The Journal of Physical Chemistry Letters* **2020**,

(23) Pépin, C.; Geneste, G.; Dewaele, A.; Mezouar, M.; Loubeyre, P. Synthesis of FeH5: A layered structure with atomic hydrogen slabs. *Science* **2017**, *357*, 382–385.

(24) Majumdar, A.; John, S. T.; Wu, M.; Yao, Y. Superconductivity in FeH 5. *Physical Review B* **2017**, *96*, 201107.

(25) Kvashnin, A. G.; Kruglov, I. A.; Semenok, D. V.; Oganov, A. R. Iron superhydrides FeH5 and FeH6: stability, electronic properties, and superconductivity. *The Journal of Physical Chemistry C* **2018**, *122*, 4731–4736.

(26) Heil, C.; Bachelet, G. B.; Boeri, L. Absence of superconductivity in iron polyhydrides at high pressures. *Physical Review B* **2018**, *97*, 214510.

(27) Wang, L.; Duan, D.; Yu, H.; Xie, H.; Huang, X.; Tian, F.; Liu, B.; Cui, T. High-Pressure Formation of Cobalt Polyhydrides: A First-Principle Study. *Inorganic Chemistry* **2017**, *57*, 181–186.

(28) Loubeyre, P.; LeToullec, R.; Hausermann, D.; Hanfland, M.; Hemley, R.; Mao, H.; Finger, L. X-ray diffraction and equation of state of hydrogen at megabar pressures. *Nature* **1996**, *383*, 702.

(29) Yoo, C.; Cynn, H.; Söderlind, P.; Iota, V. New β (fcc)-Cobalt to 210 GPa. *Physical Review Letters* **2000**, *84*, 4132.

(30) Binns, J.; Peña-Alvarez, M.; Donnelly, M.-E.; Gregoryanz, E.; Howie, R. T.; Dalladay-Simpson, P. Structural Studies on the Cu–H System under Compression. *Engineering* **2019**, *5*, 505–509.

(31) Peña-Alvarez, M.; Binns, J.; Hermann, A.; Kelsall, L. C.; Dalladay-Simpson, P.; Gregoryanz, E.; Howie, R. T. Praseodymium polyhydrides synthesized at high temperatures and pressures. *Physical Review B* **2019**, *100*, 184109.

(32) Supplemental information available at URL.

(33) Oganov, A. R.; Glass, C. W. Crystal structure prediction using ab initio evolutionary techniques: Principles and applications. *The Journal of Chemical Physics* **2006**, *124*, 244704.

(34) Glass, C. W.; Oganov, A. R.; Hansen, N. USPEX—Evolutionary crystal structure prediction. *Computer physics communications* **2006**, *175*, 713–720.

(35) Bushlanov, P. V.; Blatov, V. A.; Oganov, A. R. Topology-based crystal structure generator. *Computer Physics Communications* **2019**, *236*, 1–7.

(36) Wang, Y.; Lv, J.; Zhu, L.; Ma, Y. Crystal structure prediction via particle-swarm optimization. *Phys. Rev. B* **2010**, *82*, 094116.

(37) Wang, Y.; Lv, J.; Zhu, L.; Ma, Y. CALYPSO: A Method for Crystal Structure Prediction. *Comput. Phys. Commun.* **2012**, *183*, 2063–2070.

(38) Bazhanova, Z. G.; Oganov, A. R.; Gianola, O. Fe–C and Fe–H systems at pressures of the Earth's inner core. *Physics-Uspekhi* **2012**, *55*, 489.

(39) Yang, J. X.; Zhao, H. L.; Gong, H. R.; Song, M.; Ren, Q. Q. Proposed mechanism of HCP FCC phase transition in titianium through first principles calculation and experiments. *Sci. Rep.* **2018**, *8*, 1–9.

(40) McMillan,; L., W. Transition Temperature of Strong-Coupled Superconductors. *Physical Review* **1968**, *167*, 331–344.

(41) Allen, P. B.; Dynes, R. C. Transition temperature of strong-coupled superconductors reanalyzed. *Physical Review B* **1975**, *12*, 905–922.

(42) Li, B.; Miao, Z.; Ti, L.; Liu, S.; Chen, J.; Shi, Z.; Gregoryanz, E. Predicted high-temperature superconductivity in cerium hydrides at high pressures. *Journal of Applied Physics* **2019**, *126*, 235901.

(43) Prandini, G.; Marrazzo, A.; Castelli, I. E.; Mounet, N.; Marzari, N. Precision and efficiency in solid-state pseudopotential calculations. *Computational Materials* **2018**, *4*, 1–13.

(44) Margine, E. R.; Giustino, F. Anisotropic Migdal-Eliashberg theory using Wannier functions. *Phys. Rev. B* **2013**, *87*, 024505.

(45) Lüders, M.; Marques, M. A. L.; Lathiotakis, N. N.; Floris, A.; Profeta, G.; Fast, L.; Continenza, A.; Massidda, S.; Gross, E. K. U. Ab initio theory of superconductivity. I. Density functional formalism and approximate functionals. *Phys. Rev. B* **2005**, *72*, 024545.